

Linköping University Post Print

Time-resolved photoluminescence properties of AlGa_N/AlN/GaN high electron mobility transistor structures grown on 4H-SiC substrate

Galia Pozina, Carl Hemmingsson, Urban Forsberg, Anders Lundskog, Anelia Kakanakova-Gueorguie, Bo Monemar, Lars Hultman and Erik Janzén

N.B.: When citing this work, cite the original article.

Original Publication:

Galia Pozina, Carl Hemmingsson, Urban Forsberg, Anders Lundskog, Anelia Kakanakova-Gueorguie, Bo Monemar, Lars Hultman and Erik Janzén, Time-resolved photoluminescence properties of AlGa_N/AlN/GaN high electron mobility transistor structures grown on 4H-SiC substrate, 2008, JOURNAL OF APPLIED PHYSICS, (104), 11, 113513.

<http://dx.doi.org/10.1063/1.3028687>

Copyright: American Institute of Physics

<http://www.aip.org/>

Postprint available at: Linköping University Electronic Press

<http://urn.kb.se/resolve?urn=urn:nbn:se:liu:diva-16511>

Time-resolved photoluminescence properties of AlGaN/AlN/GaN high electron mobility transistor structures grown on 4H-SiC substrate

G. Pozina,^{a)} C. Hemmingsson, U. Forsberg, A. Lundskog, A. Kakanakova-Georgieva, B. Monemar, L. Hultman, and E. Janzén

Department of Physics, Chemistry and Biology (IFM), Linköping University, S-581 83 Linköping, Sweden

(Received 13 September 2008; accepted 10 October 2008; published online 4 December 2008)

AlGaN/AlN/GaN high electron mobility transistor heterostructures grown by metal-organic chemical vapor deposition have been studied by temperature dependent time-resolved photoluminescence. The AlGaN-related emission is found to be sensitive to the excitation power and to the built-in internal electric field. In addition, this emission shows a shift to higher energy with the reduction in the excitation density, which is rather unusual. Using a self-consistent calculation of the band potential profile, we suggest a recombination mechanism for the AlGaN-related emission involving electrons confined in the triangular AlGaN quantum well and holes weakly localized due to potential fluctuations. © 2008 American Institute of Physics.

[DOI: [10.1063/1.3028687](https://doi.org/10.1063/1.3028687)]

I. INTRODUCTION

High electron mobility transistors (HEMTs) have a broad application area, for example, in microwave and millimeter wave communication, radar, radio astronomy, monolithic microwave integrated circuits, and cell phones. AlGaN/GaN heterojunction HEMTs have many advantages in comparison with transistors based on conventional semiconductors, such as Si or GaAs. Thus, AlGaN/GaN HEMTs are presently the most attractive candidates for fabrication of high-frequency, high-power, and high-temperature microelectronic devices. A unique combination of properties, such as wide bandgap, high breakdown fields, strong polarization effects, high two dimensional electron gas (2DEG) concentration, and high saturation velocity, result in high output power density.¹ Introduction of a thin AlN exclusion layer additionally improves the room temperature sheet charge density and electron mobility of AlGaN/AlN/GaN HEMTs compared to the AlGaN/GaN heterojunctions.²

Despite improved electrical characteristics in such HEMTs,³ the influence of AlN exclusion layer on optical properties of AlGaN/AlN/GaN structures has not been sufficiently studied. In this work, we present results of time-resolved photoluminescence (TRPL) characterization performed on highly uniform 4 in. AlGaN/AlN/GaN HEMT heterostructures grown on semi-insulating 4H-SiC substrates.

II. EXPERIMENTAL

The studied HEMT structures have been grown by hot-wall metal organic chemical vapor deposition (MOCVD) technique using trimethyl gallium, trimethyl aluminum, and ammonia as precursors.⁴ A mixture of nitrogen and hydrogen has been used as carrier gas. The growth temperature was varied between 1000–1100 °C depending on the layer. Semi-insulating 4H-SiC wafers with a diameter of up to 100

mm were used as substrates. The growth of each structure was started with an 80-nm-thick AlN nucleation layer followed by a 1.8 μm thick GaN buffer layer. Target thicknesses of the thin AlN exclusion layer and of the AlGaN barrier layer were 2 and 25 nm, respectively. To get a room-temperature sheet carrier density of $1 \times 10^{13} \text{ cm}^{-2}$, the Al composition in the AlGaN alloy was adjusted to ~22%.

For photoluminescence (PL) excitation, we used the third harmonics ($\lambda_e=266 \text{ nm}$) from a Ti:sapphire femtosecond pulsed laser with a frequency of 75 MHz. TRPL measurements were performed with a Hamamatsu syncscan streak camera with a temporal resolution of ~20 ps. To disperse the PL signal we used two diffraction gratings with 150 and 1200 lines/mm. Cross-sectional transmission electron microscopy (TEM) has been made for the structural qualification of the AlGaN/AlN/GaN heterojunction using an FEI Technai G2 200 keV FEG instrument.

III. RESULTS

Typical TEM images of the structure are shown in Fig. 1. The images demonstrate the whole HEMT structure [Fig. 1(a)] and the region near the surface [Fig. 1(b)]. The interface between the GaN and AlN exclusion layers is sharp, while the boundary between AlN and AlGaN is less pronounced. We estimate that the fluctuation of the AlN thickness is in the range of 1–3 nm. The thickness of the AlGaN barrier layer has been determined by TEM measurements to ~23 nm.

The typical time-integrated low temperature PL spectrum of the investigated HEMT structures is shown in Fig. 2(a) in logarithmic scale. PL under an excitation density of 20 W/cm^2 demonstrates a broad deep-UV emission band centered at ~3.92 eV, which is related to the AlGaN layer. Another strong PL peak corresponds to the GaN excitonic transitions and includes both the neutral donor bound exciton (DX_0) line at 3.466 eV and the free exciton $A(X_A)$ emission at 3.471 eV, which means that the GaN layer is under tension.⁵ These two transitions can be clearly resolved in

^{a)}Electronic mail: galia@ifm.liu.se.

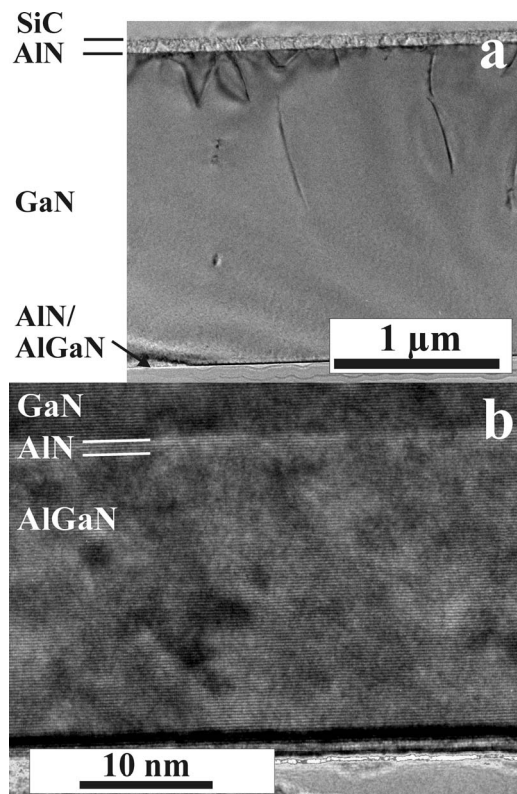


FIG. 1. TEM images of the (a) whole HEMT structure and of the (b) AlN/AlGaN interface region.

TRPL measurements performed with 1200 lines/mm grating. The two weaker emissions at ~ 3.83 and ~ 3.73 eV have the same transient, power- and temperature-dependent behavior as the 3.92 eV peak. They have also an energy shift to the 3.92 eV peak that corresponds to the longitudinal optical (LO)-phonon energy in GaN (~ 92 meV). Thus, these weaker emissions can be attributed the first and second LO-phonon replicas of the 3.92 eV band. Two additional weak PL lines at ~ 3.38 and 3.29 eV can be observed and they correspond to the LO-phonon replicas of X_A ; however, the results of the TRPL measurements presented below indicate that the 3.38 eV line might be due to overlapping between the first LO-phonon replica of X_A and the 2DEG emission.

Figure 2(b) shows a strong dependence of the AlGaN related PL band on the excitation density. Decrease in the excitation power leads to a narrowing of the PL line, i.e., the full width at half maximum is reduced from 30 meV at 20 W/cm² to 23 meV at 0.5 W/cm², which is an expected effect. On the other hand, reduction in the excitation density from 20 to 0.5 W/cm² caused a 30 meV shift in the PL maximum to higher energies. This shift has an opposite sign compared to the cases of localized exciton emission in disordered alloys or recombination from a quantum well (QW) with piezoelectric field observed for example for InGaN-based structures.^{6,7}

To elucidate the mechanism of the deep UV recombination we studied temperature dependent TRPL. Figure 3 shows low temperature (2 K) PL decay curves measured at different photon energies at two excitation densities of 6 W/cm² (black curves) and 0.5 W/cm² (gray curves). The

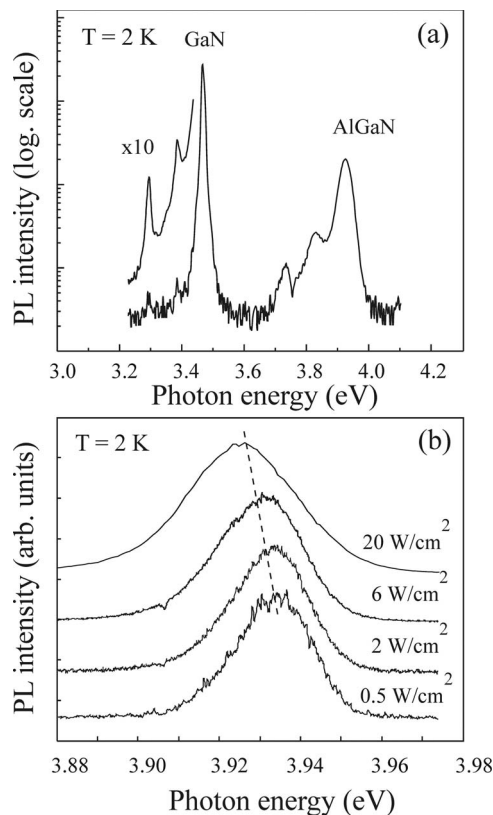


FIG. 2. (a) PL spectrum at 2 K from the AlGaN/AlN/GaN HEMT structure. (b) AlGaN-related spectra taken at different excitation densities are normalized and are vertically offset for clarity.

PL decay depends on the photon energy within the AlGaN emission. The temporal behavior of PL is qualitatively similar for both excitation densities and can be characterized by a fast nonexponential decay with characteristic decay time (τ) of ~ 100 ps for the high-energy spectral side, whereas for the lower energy spectral side, the emission demonstrates a slow near exponential kinetics with a decay time of ~ 700 – 1000 ps. This temporal behavior may be expected from the recombination of localized and spatially separated carriers. In order to get further insight on the origin of the

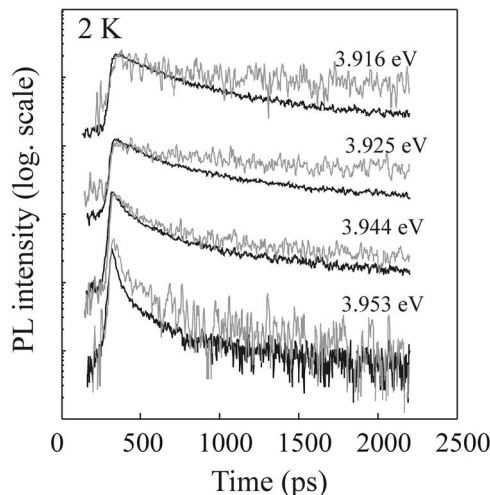


FIG. 3. PL decay curves measured within the AlGaN emission band at the excitation density of 6 W/cm² (black lines) and 0.5 W/cm² (gray lines).

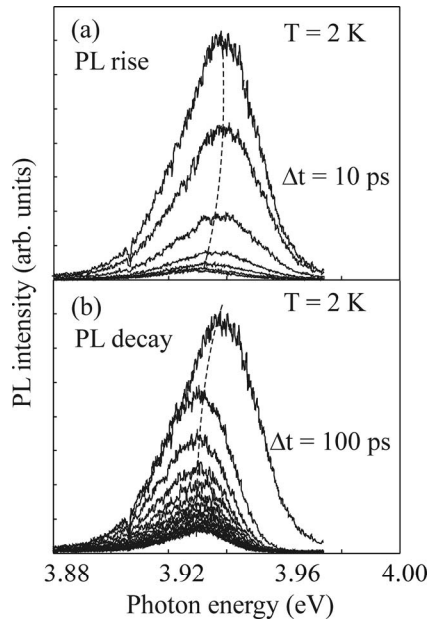


FIG. 4. TRPL spectra measured at the excitation density of 6 W/cm^2 during the (a) PL rise and (b) decay.

3.92 eV peak, we studied the details of the transient PL. Figure 4 shows the AlGa_N related recombination after the laser pulse during the PL rise [Fig. 4(a)] and during the PL decay [Fig. 4(b)]. The emission peak shows a higher energy shift of $\sim 5 \text{ meV}$ during the rise and a lower energy shift of $\sim 6 \text{ meV}$ during the decay. This is a doubtless indication that the AlGa_N related PL likely originated from the recombination of carriers confined in a quantum-well-like potential.

On the other hand, the temperature dependent TRPL demonstrated that the PL decay time for the AlGa_N related transition decreases very fast. Already at 50 K, the thermalization is practically complete as can be seen in Fig. 5, where

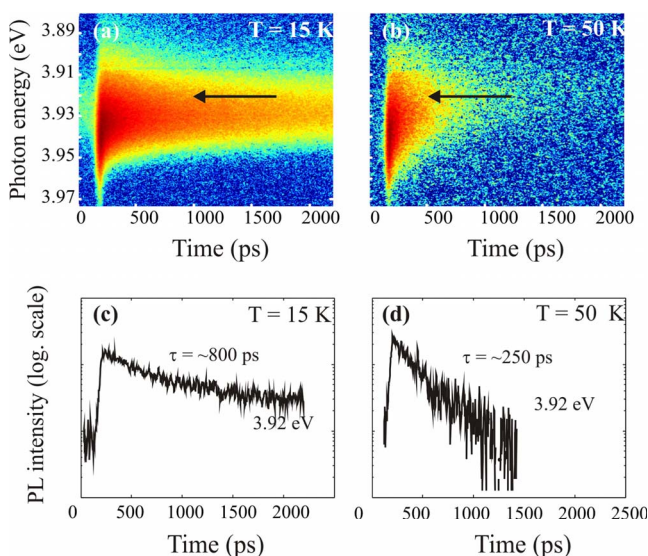


FIG. 5. (Color online) TRPL images measured at (a) 15 and (b) 50 K. Arrows indicate the energy position of 3.92 eV, where the PL decay curve has been taken at (c) 15 and (d) 50 K.

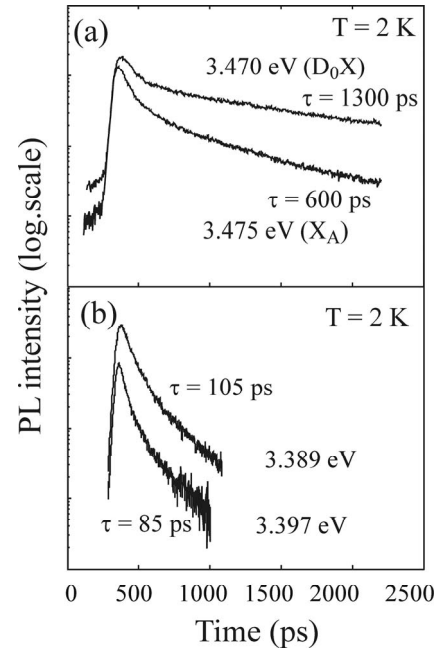


FIG. 6. (a) PL decay curves for the D_0X and X_A transitions taken at 2 K and excitation density 20 W/cm^2 . (b) PL decay curves for the LO-phonon replica of X_A (two photon energies at 3.389 and 3.397 eV are chosen for illustration).

two TRPL images measured at elevated temperatures of 15 [Fig. 5(a)] and 50 K [Fig. 5(b)] are shown as examples. The PL decay curves taken at the selected photon energy of 3.92 eV are shown in Figs. 5(c) and 5(d) for 15 and 50 K, respectively. In the temperature range of 2–15 K, the PL decay at the photon energy of 3.92 eV is slow and almost constant. However, at higher temperatures than 30 K the decay time is drastically reduced. This thermal quenching of the AlGa_N related emission occurs at a lower temperature than the thermal quenching of the GaN-related excitonic emissions and suggests a very weak localization of carriers in the AlGa_N layer. A possible explanation of this behavior will be discussed later after the calculation results of the band structure are presented.

In stationary PL under continuous wave excitation conditions the 2DEG transition can hardly be seen. However, using an fs pulse excitation of high average density we demonstrated that the weak emission at $\sim 3.38\text{--}3.39 \text{ eV}$ might be related to the 2DEG. This weak band is likely an overlapping of the first LO phonon replica of the X_A transition and the 2DEG emission, as can be seen in TRPL. Figure 6(a) shows the PL decay curve measured for the X_A and for the D_0X transitions. Two exponential processes can describe the PL decay curves where after about 200 ps the slowest process dominates. Fitting to the slowest process gives a decay time of $\tau=600 \text{ ps}$ and $\tau=1300 \text{ ps}$ for the X_A and for the D_0X lines, respectively. At the same time, one can see in Fig. 6(b) that the 3.39 eV transition has a much shorter recombination time as compared to the no-phonon (NP) exciton transitions. The PL decay time varies between 50 and 80 ps within this band [as indicated in Fig. 6(b)] and is faster for the higher energy and slower for the lower energy spectral

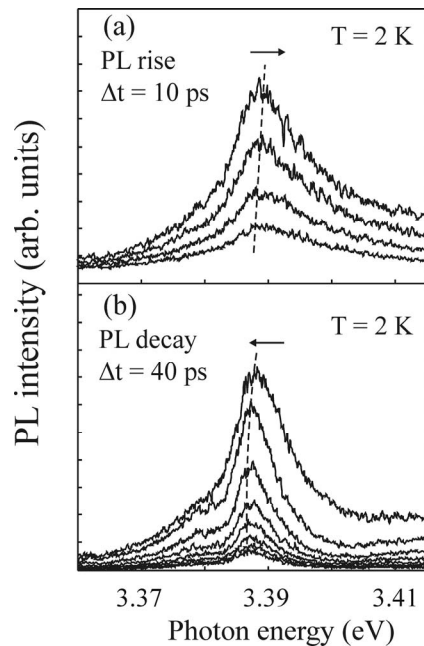


FIG. 7. TRPL spectra taken at the excitation density of 20 W/cm² shown (a) with time separation of 10 ps during the PL rise and (b) with time separation of 40 ps during the PL decay.

side. The decay time is expected to be the same or longer for the phonon replicas in comparison with NP lines as it was previously reported for GaN.^{8,9}

In addition, the 3.39 eV shows in TRPL a higher energy shift of ~ 2 meV under the PL rise process [see Fig. 7(a)] and a low energy shift of the same order under the PL decay [Fig. 7(b)]. This observation is a strong argument that the 3.39 eV emission is sensitive to a built-in internal electric field and consequently might be associated with the 2DEG.

IV. MODEL AND DISCUSSION

In order to understand the PL and TRPL observations the band potential profile in our HEMT structure was calculated based on a self-consistent solution of the Schrödinger and Poisson equations. It was found that a triangular potential well is formed in the AlGa_{0.22}N layer and if the AlN thickness was less than 2 nm and if the surface potential exceeds 0.9 eV, electrons can be confined in the triangular QW. The result of calculations for one typical case with an AlN thickness of 1 nm and with a surface potential of 1.2 eV is illustrated in Fig. 8. A thickness of 1 nm is a realistic choice based on the analysis of the TEM results. In the calculations, we assumed a temperature of 4 K and that the HEMT structure is undoped. Based on these assumptions, the parameters used for the calculation are presented in Table I. Figure 8 also shows the envelope function of electrons confined in the triangular AlGa_{0.22}N QW and at the interface between the AlN and GaN. We also indicated in Fig. 8 the ground and the second subbands occupied by 2DEG. From the calculations we obtain a sheet electron density of 1.73×10^{13} cm⁻², which is about 70% higher than the measured value at room temperature. It is important to point out here that according

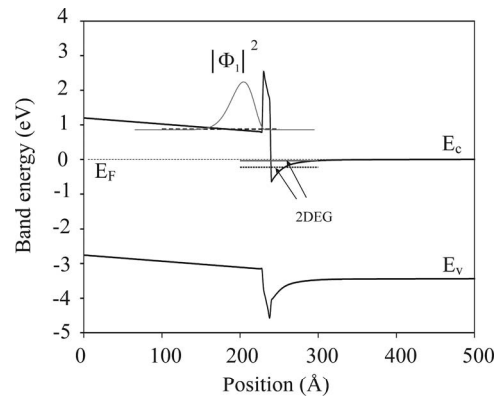


FIG. 8. Self-consistent calculation of band diagram using parameters from Table I. AlN thickness in this case is 1 nm. One energy state with $E_1 = 0.88$ eV from the Fermi level is found in the triangular AlGa_{0.22}N QW. The electron envelope function is shown for this QW. Two energy subbands for 2DEG in GaN are also found in this case. The states for 2DEG are below the Fermi level with energies $E_1 = -0.22$ eV and $E_2 = -0.03$ eV.

to our calculations there is no hole localization in the band potential neither in AlGa_{0.22}N nor in GaN layers for any reasonable parameters.

It is known in AlGa_{0.22}N alloys grown by MOCVD that there are random fluctuations in the potential due to alloy fluctuations^{16–18} and this gives rise to carrier localization. Thus, taking into account results of the TRPL measurements and the calculated band structure, we suggest that the AlGa_{0.22}N related emission likely occurred between electrons strongly confined in the triangular AlGa_{0.22}N QW and holes weakly localized on potential fluctuations. Schematically, this model is shown in Fig. 9; only the valence band is enlarged in the figure. The electrons and holes are spatially separated, which explains the rather long PL recombination times and the dependence of τ on the photon energy. This model is in agreement (i) with the observed energy shifts after laser pulse during the PL rise and PL decay, (ii) with the higher energy shift of the time-integrated PL peak under reduction in the excitation power, and (iii) with the thermal quenching at relatively low temperatures of the AlGa_{0.22}N-related PL. The first effect can be understood in terms of sensitivity of the electron level in the triangular QW to the potential profile and to a built-in electric field. The second phenomenon can be explained by the narrowing of the triangular QW under the reduced excitation power when the screening effect is weaker. In this case the electron energy level is shifted to higher energies. Finally, the third effect, thermal quenching at 35–40 K confirms a very weak hole confinement with the

TABLE I. Parameters at 4 K used for self-consistent calculation.

Material	GaN	AlN	Al _{0.22} Ga _{0.78} N	References
Bandgap E_g (eV)	3.44	6.25	3.955	9 and 10
Conduction band offset (eV)	0	2.1075	0.38625	11
Dielectric constant	10.28	10.31	10.287	12
Piezoelectric field (C/m ²)	0	-0.0525	-0.00671	13
Spontaneous polarization (C/m ²)	-0.0427	-0.09	-0.0427	13
Effective electron mass	0.22	0.33	0.244	14 and 15

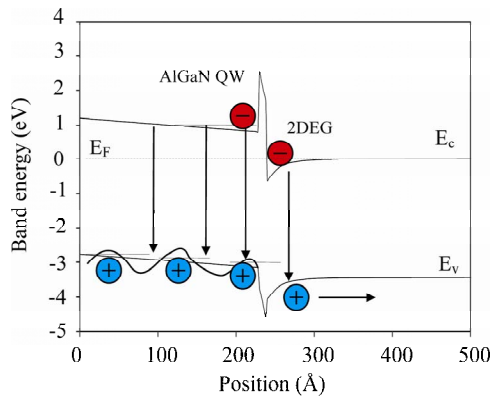


FIG. 9. (Color online) Schematic model shows possible transitions between electrons confined in the triangular AlGaIn QW and holes localized on potential fluctuations.

localization energy of the order of 4–5 meV. This quenching cannot be explained by the increased contribution of nonradiative recombination channels, since the GaN related emission is still not noticeably affected at these temperatures.

Concerning the 3.39 eV emission, since it is sensitive to the built-in electric field, it is associated to the 2DEG formed in the interface between the AlN and the GaN. The short decay time can be explained from the fact that photogenerated holes are quickly swept away from the 2DEG region into the flat band region where there is no overlapping between electron and holes wave functions. Thus, the decay time is determined by the transfer time of holes from the 2DEG region.

V. CONCLUSIONS

We have studied AlGaIn/AlN/GaN HEMT heterostructures grown on a semi-insulating 4H-SiC substrate by MOCVD. PL measurements at 2 K demonstrate a broad emission band at 3.8–3.9 eV originating from the AlGaIn layer, and an exciton related transition at ~ 3.46 eV originating from the GaN layer. TRPL studies reveal that the AlGaIn-related emission shows energy shifts of opposite sign during the PL rise and PL decay, respectively. In addition, the AlGaIn-related emission demonstrates a higher energy shift with decreasing excitation power and a fast thermal quenching at $T > 35$ –40 K. The weak emission at ~ 3.38 –3.39 eV, i.e., at an energy which corresponds to the LO phonon rep-

lica of exciton, is sensitive to a built-in internal electric field and consequently is likely an overlapping between the first LO phonon replica of X_A in GaN and the 2DEG transition. Based on a self-consistent calculation we explained the mechanism responsible for the deep UV PL in AlGaIn by recombination of electrons strongly confined in the triangular AlGaIn QW and by holes weakly localized on random alloy potential fluctuations.

ACKNOWLEDGMENTS

This work was supported by the Swedish Research Council (VR), the Swedish Energy Agency, and the Swedish Foundation for Strategic Research (SSF).

- ¹Y.-F. Wu, D. Kapolnek, J. P. Ibbetson, P. Parikh, B. P. Keller, and U. K. Mishra, *IEEE Trans. Electron Devices* **48**, 586 (2001).
- ²L. Shen, S. Heikman, B. Moran, R. Coffie, N.-Q. Zhang, D. Buttari, I. P. Smorchkova, S. Keller, S. P. DenBaars, and U. K. Mishra, *IEEE Electron Device Lett.* **22**, 457 (2001).
- ³A. Lundskog, U. Forsberg, A. Kakanakova-Georgieva, R. Ciechonski, I. G. Ivanov, V. Darakchieva, E. Janzén, M. Fagerlind, J.-Y. Shiu, and N. Rorsman, Proceedings of the ICNS-7, Las Vegas, Nevada, 2007 (unpublished).
- ⁴A. Kakanakova-Georgieva, U. Forsberg, I. G. Ivanov, and E. Janzén, *J. Cryst. Growth* **300**, 100 (2007).
- ⁵G. Pozina, N. V. Edwards, J. P. Bergman, T. Paskova, B. Monemar, M. D. Bremser, and R. F. Davis, *Appl. Phys. Lett.* **78**, 1062 (2001).
- ⁶G. Pozina, J. P. Bergman, B. Monemar, T. Takeuchi, H. Amano, and I. Akasaki, *J. Appl. Phys.* **88**, 2677 (2000).
- ⁷G. Pozina, J. P. Bergman, B. Monemar, M. Iwaya, S. Nitta, H. Amano, and I. Akasaki, *Appl. Phys. Lett.* **77**, 1638 (2000).
- ⁸B. Monemar, P. P. Paskov, J. P. Bergman, A. A. Toropov, and T. V. Shubina, *Phys. Status Solidi* **244**, 1759 (2007) (b).
- ⁹B. Monemar, P. P. Paskov, J. P. Bergman, A. A. Toropov, T. V. Shubina, T. Malinauskas, and A. Usui, *Phys. Status Solidi B* **245**, 1723 (2008).
- ¹⁰Q. Guo, A. Yoshida, *Jpn. J. Appl. Phys., Part 1* **33**, 2453 (1994).
- ¹¹A. Sher, M. van Schilfgaarde, M.A. Berding, S. Krishnamurthy and A.-B. Chen, *MRS Internet J. Nitride Semicond. Res.* **4S1**, G5.1 (1999).
- ¹²G. Martin, A. Botchkarev, A. Rockett, and H. Morkoc, *Appl. Phys. Lett.* **68**, 2541 (1996).
- ¹³F. Bernardini and V. Fiorentini, *Phys. Rev. Lett.* **79**, 3958 (1997).
- ¹⁴O. Ambacher, J. Majewski, C. Miskys, A. Link, M. Hermann, M. Eichhoff, M. Stutzmann, F. Bernardini, V. Fiorentini, V. Tilak, B. Schaff, and L. F. Eastman, *J. Phys.: Condens. Matter* **14**, 3399 (2002).
- ¹⁵K.-S. Lee, D.-H. Yoon, S.-B. Bae, M.-R. Park, and G.-H. Kim, *ETRI J.* **24**, 270 (2002).
- ¹⁶Y.-H. Cho, G. H. Gainer, J. B. Lam, and J. J. Song, *Phys. Rev. B* **61**, 7203 (2000).
- ¹⁷A. Bell, S. Srinivasan, C. Plumlee, H. Omiya, F. A. Ponce, J. Christen, S. Tanaka, A. Fujioka, and Y. Nakagawa, *J. Appl. Phys.* **95**, 4670 (2004).
- ¹⁸E. Kuokstis, W. H. Sun, M. Shatalov, J. W. Yang, and M. Asif Khan, *Appl. Phys. Lett.* **88**, 261905 (2006).